Temporally controlled targeted somatic mutagenesis in embryonic surface ectoderm and fetal epidermal keratinocytes unveils two distinct developmental functions of BRG1 in limb morphogenesis and skin barrier formation

Arup Kumar Indra[1,2], Valérie Dupé[1], Jean-Marc Bornert[1], Nadia Messaddeq[1], Moshe Yaniv[4], Manuel Mark[1,2], Pierre Chambon[2,3,*] and Daniel Metzger[1,2,*]

[1]Institut de Génétique et de Biologie Moléculaire et Cellulaire (IGBMC), CNRS, INSERM, ULP, BP 10142-67404, Illkirch, C.U. de Strasbourg, France
[2]Institut Clinique de la Souris (ICS), BP 10142, CU de Strasbourg, 67404 Illkirch, France
[3]Collège de France, 11 Place Marcelin Berthelot, 75231 Paris Cedex 05, France
[4]Unité Expression Génétique et Maladies, CNRS URA 1644, Département de Biologie du Développement, Institut Pasteur, 75724 Paris, France
*Authors for correspondence (e-mail: metzger@igbmc.u-strasbg.fr and chambon@igbmc.u-strasbg.fr)

Accepted 1 August 2005

Development 132, 4533-4544
Published by The Company of Biologists 2005
doi:10.1242/dev.02019

Summary

Animal SWI2/SNF2 protein complexes containing either the brahma (BRM) or brahma-related gene 1 (BRG1) ATPase are involved in nucleosome remodelling and may control the accessibility of sequence-specific transcription factors to DNA. In vitro studies have indicated that BRM and BRG1 could regulate the expression of distinct sets of genes. However, as mice lacking BRM are viable and fertile, BRG1 might efficiently compensate for BRM loss. By contrast, as *Brg1*-null fibroblasts are viable but *Brg1*-null embryos die during the peri-implantation stage, BRG1 might exert cell-specific functions. To further investigate the in vivo role of BRG1, we selectively ablated *Brg1* in keratinocytes of the forming mouse epidermis. We show that BRG1 is selectively required for epithelial-mesenchymal interactions in limb patterning, and during keratinocyte terminal differentiation, in which BRM can partially substitute for BRG1. By contrast, neither BRM nor BRG1 are essential for the proliferation and early differentiation of keratinocytes, which may require other ATP-dependent nucleosome-remodelling complexes. Finally, we demonstrate that cell-specific targeted somatic mutations can be created at various times during the development of mouse embryos cell-specifically expressing the tamoxifen-activatable Cre-ER^{T2} recombinase.

Key words: Targeted somatic mutagenesis, Cre-Lox, Epidermis, Limb, SNF2β-BRG1.

Introduction

In eukaryotes, genes are packaged into chromatin structures that can be modulated to generate transcriptionally active or repressed configurations. Regulation of gene expression requires interplay between the transcription machinery and the multisubunit protein complexes that remodel chromatin structures, thereby controlling the accessibility of sequence-specific transcription factors to individual genes. Such complexes either covalently modify histones or DNA, or disrupt histone-DNA contacts through ATP-dependent nucleosome remodeling. ATP-dependent nucleosome remodeling complexes contain a number of subunits, including an ATPase of the SNF2 family. Several subfamilies (e.g. SWI2/SNF2, ISWI and Mi-2) of the SNF2 family have been identified in various species, based on the identity of their catalytic ATPase subunit. SWI2/SNF2, one of the best characterised remodeling complex subfamilies, was first identified in yeast, and is highly conserved among eukaryotes. Animal SWI2/SNF2 complexes contain one of the two ATPases, BRG1 (SNF2β) or BRM (SNF2α), and a variable subunit composition of BRG1-associated factors (BAFs) (Eberharter and Becker, 2004).

As mice lacking BRM are viable and fertile (Reyes et al., 1998), it was suggested that BRM and BRG1 might be functionally redundant. However, in vitro studies indicated that the two factors might each be involved in regulating the expression of different sets of genes (Kadam and Emerson, 2003). Moreover, *Brg1* ablation in murine F9 embryonal carcinoma cells results in cell death, thus demonstrating that BRG1 plays crucial, non-redundant functions (Sumi-Ichinose et al., 1997). However, it is not a general cell viability factor, as *Brg1*-null mouse fibroblasts are viable (Bultman et al., 2000). Lethality of *Brg1*-null mouse embryos during the peri-implantation stage demonstrated that BRG1 exerts specific functions early in development, but precluded the elucidation of its function(s) at later stages in mammals (Bultman et al., 2000). Interestingly, Cre-

mediated ablation of *Brg1* during T cell development revealed essential roles of this factor at various stages of T cell differentiation (Chi et al., 2003).

The skin, which consists of the epidermis and underlying dermis, is a very attractive tissue in which to study the in vivo functions of genes that regulate the expression of proteins involved in the control of cellular proliferation and differentiation. During embryonic development, the ectodermal cell layer covering the body develops into a stratified epidermis that is essential at birth, when the organism confronts the arid and toxic postnatal environments. The first sign of stratification of mouse embryonic epidermis occurs at embryonic day (E) 9.5, when the periderm forms. Epidermal maturation continues with the formation of the future spinous layer at E15.5, and by E18.5 the epidermis is fully differentiated (Byrne et al., 2003). Keratinocytes from the basal layer periodically withdraw from the cell cycle and commit to terminal differentiation, while migrating to the next layers. The outermost layer of the skin (statum corneum) is composed of mechanically tough, dead, cornified cells (squames), which develop as a result of a complex terminal differentiation program, and provide vital physical and permeability barriers to vertebrates (Kalinin et al., 2002). Formation of the epidermal permeability barrier requires the delivery of lipids and proteins, which are contained in lamellar granules (keratinosomes) present in keratinocytes of the granular layer, to the stratum corneum interstices, as well as the formation of high molecular weight polymers through the crosslinking of corneocyte envelope proteins (loricrin, involucrin, filagrin and other peptides) and packing of corneocytes by corneodesmosomes. Epidermal homeostasis relies on a tightly regulated balance between keratinocyte proliferation and differentiation, the alteration of this leads to various skin diseases (Watt, 2000).

To investigate the role of BRG1 in skin ontogenesis, we established mice bearing LoxP-flanked (floxed) *Brg1* alleles and ablated *Brg1* in the forming epidermis using K14-Cre (Li et al., 2001) or K14-Cre-ER^{T2} (Indra et al., 2000; Li et al., 2000) transgenic mice that express either the bacteriophage P1 Cre-recombinase or the ligand-dependent Cre-ER^{T2} recombinase under the control of the human K14 promoter, which is active in the surface ectoderm and the basal layer of the epidermis (Vassar et al., 1989). We show that BRG1 is dispensable for embryonic epidermis formation, but is essential for establishing the skin barrier at later fetal stages. Ablation of *Brg1* in the forming epidermis before E12.5 also induces developmental limb defects that are by-passed by temporally controlled *Brg1* ablation at later times. Moreover, ablation of *Brg1* in epidermal keratinocytes of mice lacking BRM revealed that the SWI2/SNF2 ATPase subunits of the chromatin remodelling complexes are not essential for keratinocyte proliferation and 'early' differentiation, and that BRM can partially substitute for BRG1 function during keratinocyte 'late' terminal differentiation.

Materials and methods

Mice

Brg1$^{L2/L2}$ mice were generated through homologous recombination in ES cells using the pSNF2β$^{L:LHLa}$ targeting vector (Sumi-Ichinose et al., 1997). P1 embryonic stem (ES) cell electroporation, selection of hygromycin-resistant clones, Cre-mediated excision and Southern blot analysis were performed as described previously (Dierich and Dollé, 1997; Sumi-Ichinose et al., 1997). *K14-Cre* and *K14-Cre-ER*^{T2} transgenic mice, *RosaR26R Cre*-reporter mice and *Brm* null mice were described (Indra et al., 1999; Li et al., 2001; Reyes et al., 1998; Indra et al., 2000; Li et al., 2000; Soriano, 1999).

Tamoxifen administration

Tam (0.1 mg in 50 μl sunflower oil), prepared as described (Metzger et al., 2003), and oil (vehicle) were injected intraperitonially to pregnant females.

Genotyping of *Brg1* alleles

Genomic DNA was isolated from fetal skin and adult tail skin, and, whenever required, the dermis and epidermis was separated (Li et al., 2001). The various *Brg1* alleles were identified by PCR with P1, P2 and P3 primers: (+) allele, P1-P2 (241 bp); (L2) allele, P1-P2 (387 bp); (L–) allele, P3-P2 (313 bp) (Sumi-Ichinose et al., 1997).

X-Gal staining, in situ RNA analysis and skeletal analysis

For whole-mount X-Gal staining, embryos recovered between E9.5 and E10.5 were fixed in 2% formaldehyde, rinsed in PBS (pH 7.4) and incubated in 5-bromo-4-chloro-3-indolyl-β-D-galactopyranoside (X-Gal) solution in PBS overnight at 37°C in the dark (Byrne et al., 1994), washed twice in PBS and photographed. X-Gal staining of 10 μm thick frozen sections was performed as described (Indra et al., 1999). Whole-mount *Fgf8* in situ hybridization was as described (Wendling et al., 2001). Skeletons of E18.5 fetuses were prepared and stained as described (Lufkin et al., 1992).

Semithin and electron microscopic analysis

Limb buds were collected from E11.5 foetuses. Skin biopsies were matched for age and body sites. Semithin (2 μm section) and transmission electron microscopy samples were processed as described (Li et al., 2001; Segre et al., 1999). For scanning electron microscopy (SEM), samples were prepared as described (Choi et al., 1997).

Immunohistochemistry

After fixation in 2% paraformaldehyde (PFA), 10 μm skin or limb cryosections were blocked in 5% normal goat serum (NGS, Vector), incubated overnight with a polyclonal rabbit anti-BRG1 antibody (1:1000) at 4°C (Sumi-Ichinose et al., 1997), washed in PBS/0.1% Tween 20, and incubated for 1 hour at room temperature with a CY3-conjugated donkey anti-rabbit antibody (1:400) (Jackson ImmunoResearch) or an Alexa-conjugated goat anti-rabbit antibody (1:200) (Interchim, France). BRM and KI-67 immunohistochemistry was performed on 10 μm dorsal skin cryosections as decribed (Reyes et al., 1998; Li et al., 2001). Counterstaining was performed with DAPI.

Skin permeability assay

X-Gal permeability was performed according to Hardman et al. (Hardman et al., 1998). Briefly, freshly isolated E18.5 fetuses were rinsed in PBS, immersed in X-Gal solution, pH 4.5, at 37°C for 8 hours, washed in PBS for 1-2 minutes and photographed.

In vivo transdermal absorption of the fluorescent dye Lucifer yellow

E18.5 fetuses were restrained in Petri dishes with their backs in contact with 1 mM Lucifer Yellow in PBS (pH 7.4) at 37°C, as described (Matsuki et al., 1998). After a 1-hour incubation, fetuses were sacrificed, frozen and cryosectioned dorsoventrally at a thickness of 5 μm. DAPI counterstained sections were analysed by fluorescence microscopy.

Trans-epidermal water loss (TEWL) measurement

Dorsal and ventral skin TEWL was determined on E18.5 fetuses with

a Cortex Technology's Dermalab system (Denmark), equipped with a TEWL probe. Mean values of six measurements per animal were determined. Data are expressed in g/h/m^2, as means±s.e.m. from four animals.

Quantitative RT-PCR

Total RNA was extracted from approximately 100 mg skin of E18.5 fetuses using Trizol® Reagent (GIBCO BRL Life technologies). cDNA was synthesised from 5 μg RNA using the Superscript™ II kit (Invitrogen) according to the manufacturer's instructions. Real-time PCR was performed with a LightCycler (Roche Diagnostics) and the SYBR green kit. For that purpose, 5 μl of cDNA was diluted to 20 μl, and 2 μl of the diluted cDNA was used for each amplification. Amplification specificity was verified by melting-curve analysis and the data quantified with the LightCycler software. Alternatively amplified products from the exponential phase (between 20-25 cycles) were electrophoresed on 2% agarose gel, transferred onto nylon membrane and probed with radiolabelled oligonucleotides. Primers used were as follows.

TGase1, 5′-AACGACTGCTGGATGAAGAG-3′ (sense; S) and 5′-CTGCCAGTATACCTTATCGCT-3′ (antisense; As);

TGase3, 5′-TACACACTGAGTGTTGAGATC-3′ (S) and 5′-AGAGGCTGATGTTCAGAATGT-3′ (As);

KLF4, 5′-CATTATCAAGAGCTCATGCCA-3′ (S) and 5′-GT-CACAGTGGTAAGGTTTCTC-3′ (As);

claudin, 5′-GTGGAAGATTTACTCCTATGC-3′ (S) and 5′-CAGGATGCCAATTACCATCAA-3′ (As);

corneodesmosin, 5′-TGCTGATGGCCGGTCTTATTC-3′ (S) and 5′-ACCTTGGCTGCTGATGCTGTT-3′ (As); and

HPRT, 5′-GTAATGATCAGTCAACGGGGGAC-3′ (S) and 5′-CCAGCAAGCTTGCAACCTTAACCA-3′ (As).

The radiolabeled oligonucleotide probes were:

TGase1, 5′-GAGACCAGCAGTGGCATCTTCTGCTGTGGC-3′;

TGase3, 5′-ATGAGTAACCACGCCGAAAGACAAGAGTAT-3′;

KLF4, 5′-TCTCATCTCAAGGCACACCTGCGAACTCAC-3′;

claudin 1, 5′-AATCTGAACAGTACTTTGCAGGCAACC-3′; and

HPRT, 5′-GCTTTCCCTGGTTAAGCAGTACAGCCCC-3′.

Statistical analyses

Where relevant, data were compared by Unpaired Student's *t*-test, with corrections for unequal variance made using the Statview 5 programme (Abacus Concepts, CA, USA). Values are reported as mean±s.e.m. and the significance level was set at P=0.05.

Results

Generation of mice bearing floxed *Brg1* alleles

To generate a conditional-null mutation of the *Brg1* (SNF2β) gene in the mouse, ES cells were electroporated with the targeting vector pSNF2β$^{L:LHLa}$ (Sumi-Ichinose et al., 1997) bearing a loxP site upstream of *Brg1* exon 2 and a loxP-flanked hygromycin-resistance cassette inserted in the intron located downstream of exon 3 (Fig. 1A). Screening of 240 ES clones by Southern blotting and PCR analysis yielded two ES clones with one targeted *Brg1* L3 allele (Fig. 1A,B; and data not shown). These two *Brg1*$^{L3/+}$ ES lines were then transiently transfected with a Cre-expression vector, and *Brg1*$^{L2/+}$ ES cells in which the loxP-flanked selection marker was selectively excised were identified (Fig. 1A,B, and data not shown). Males derived from two independent *Brg1*$^{L2/+}$ ES clones transmitted the floxed allele through their germline. Heterozygous and homozygous *Brg1* L2 mice were indistinguishable from their wild-type littermates (data not shown).

Efficient *Brg1* ablation in the limb ectoderm before E11.5 and in epidermal keratinocytes of *K14-Cre*$^{tg/0}$/*Brg1*$^{L2/L2}$ fetuses during skin morphogenesis

We have previously shown that the Cre recombinase expressed under the control of the human *K14* promoter in *K14-Cre* transgenic mice efficiently mediates site-specific recombination at loxP sites in keratinocytes of fetal and adult epidermis (Li et al., 2001). To further characterise Cre activity during skin ontogenesis, hemizygote *K14-Cre*$^{tg/0}$ mice were bred with *RosaR26R* reporter mice (called thereafter *ROSA*$^{fl/+}$) that express β-galactosidase after Cre-mediated recombination (Soriano, 1999). In E9.5 *K14-Cre*$^{tg/0}$/*ROSA*$^{fl/+}$ bigenic fetuses, X-Gal staining was patchy, but mainly located in the caudal region and forming forelimb bud (Fig. 1C, compare parts a and b). By E10, it was still restricted to the posterior region of the embryo and limb buds (Fig. 1C, part c, and data not shown). Note that staining of the 'forming' hindlimb bud appeared stronger than that of the forelimb bud. Histological analyses revealed that Cre-mediated excision was restricted to the ectodermal layer (data not shown). At E12.5, X-Gal staining was uniformly distributed in the surface ectoderm, including that of limbs, and after E14.5 most, if not all, epidermal keratinocytes were X-Gal stained (Fig. 1D, and data not shown).

Immunohistochemical analysis of E10.5, E11.0 and E12.5 control embryos revealed that BRG1 was uniformly expressed in the surface ectoderm, including that of outgrowing limbs (Fig. 2A,B, and data not shown). At E18.5, it was strongly expressed in most, if not all, basal cells, as well as in about 70% of the spinous and 30% of the granular cells (Fig. 2C, parts a and b, and data not shown). To ablate *Brg1* in the forming epidermis, *Brg1*$^{L2/L2}$ mice were bred with *K14-Cre*$^{tg/0}$ mice, to generate *K14-Cre*$^{tg/0}$/*Brg1*$^{L2/L2}$ fetuses. L$^-$, but no L2, alleles were detected in the epidermis of E18.5 *K14-Cre*$^{tg/0}$/*Brg1*$^{L2/L2}$ fetuses, whereas only L2 alleles were present in their dermis (see Fig. 2D, lanes 1 and 2), thus demonstrating that *Brg1* was efficiently and selectively ablated in keratinocytes of the forming epidermis. In agreement with these results, no BRG1 protein was revealed by immunohistochemistry in epidermal keratinocytes of E18.5 *K14-Cre*$^{tg/0}$/*Brg1*$^{L2/L2}$ fetuses [hereafter called *Brg1*$^{ep-/-(c)}$ mice] (Fig. 2C, parts c and d). Note that *Brm* transcript levels were similar in the skin of E18.5 control and *Brg1*$^{ep-/-(c)}$ fetuses (data not shown). At E10.5, the BRG1 protein expression pattern was similar in the surface ectoderm of *Brg1*$^{L2/L2}$ (control) and *Brg1*$^{ep-/-(c)}$ fetuses, but, at E11, BRG1 was decreased in the cells of the surface ectoderm of *Brg1*$^{ep-/-(c)}$ forelimbs and was very low in mutant hindlimbs (Fig. 2A; and data not shown). At E11.5, BRG1 protein was not detected in either fore- or hindlimb ectoderm (data not shown). Moreover, BRG1 protein was observed in less than 50% of the cells of the dorsal ectoderm of E11.5 *Brg1*$^{ep-/-(c)}$ fetuses, and, at E12.5, almost all ectodermal cells were BRG1-depleted (Fig. 2B; and data not shown). Thus, *Brg1* is efficiently ablated in the limb ectoderm at E11.5, and in the developing epidermis of *Brg1*$^{ep-/-(c)}$ fetuses before E12.5.

Brg1 ablation in the limb ectoderm of *Brg1*$^{ep-/-(c)}$ fetuses induces severe hindlimb defects

E18.5 *Brg1*$^{ep-/-(c)}$ mutant fetuses were obtained at the expected

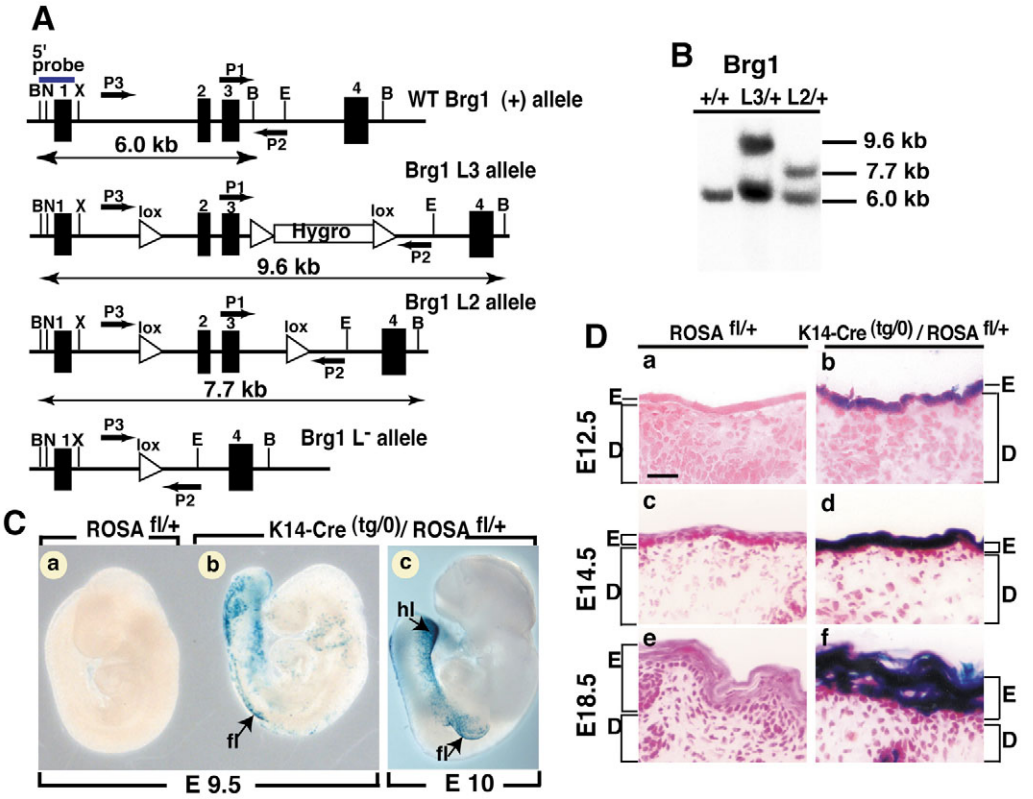

Fig. 1. Generation of mice harboring floxed *Brg1* alleles and characterisation of the Cre activity of *K14-Cre* mice during embryogenesis. (A) Targeting strategy of the mouse *Brg1* locus. Partial structure of the *Brg1* locus [*Brg1* (+) allele]. Exons are indicated by black boxes. The *Brg1* L3 allele containing the three loxP sites (lox) and the hygromycin resistance marker (Hygro) is presented. The expected genomic maps after excision of the floxed marker (*Brg1* L2 allele) and excision of both the marker and exons 2 and 3 (*Brg1* L^- allele) are shown. The arrows indicate the PCR primer location (P1-P3). The location of the Southern blot 5′-probe (Sumi-Ichinose et al., 1997) is shown. The size of DNA segments obtained after *Bam*HI restriction digest and detection with the 5′-probe are indicated. B, *Bam*HI; N, *Nhe*I; X, *Xba*I; E, *Eco*RV. (B) Southern blot analysis of genomic DNA isolated from $Brg1^{+/+}$, $Brg1^{L3/+}$ and $Brg1^{L2/+}$ ES cells, digested by *Bam*HI and hybridized with the 5′ probe. (C) Whole-mount X-Gal stained E9.5 (a,b) and E10.0 (c) control $ROSA^{fl/+}$ (a) and $K14\text{-}Cre^{tg/0}/ROSA^{fl/+}$ (b,c) embryos. fl, forelimb; hl, hindlimb. (D) X-Gal-stained dorsal skin sections from E12.5 (a,b), E14.5 (c,d) and E18.5 (e,f) control $ROSA^{fl/+}$ (a,c,e) and $K14\text{-}Cre^{tg/0}/ROSA^{fl/+}$ (b,d,f) fetuses. Sections were counterstained with safranin. E, epidermis; D, dermis. Scale bar in a: 24 μm.

mendelian ratio. Their forelimbs were properly developed, but their hindlimbs and tails were malformed (Fig. 3A, and data not shown). The severity of the hindlimb defects was variable, ranging from five abnormal digits and a normal zeugopod (tibia and fibula), to a malformed single digit and absence of the tibia (Fig. 3B; see also Table S1 in the supplementary material). The most proximal element of the hindlimb, the stylopod (femur), was always normal. As similar distal truncations were previously observed in chick limb Apical Ectodermal Ridge (AER) extirpation studies (Summerbell, 1974), we examined the consequences of *Brg1* ablation on the AER. To this end, we analysed the expression of *Fgf8*, which is both a marker of the AER and a key mediator of its organizing functions along the proximodistal axis (Moon and Capecchi, 2000; Sun et al., 2002). *Fgf8* was similarly expressed in the AER of control and $Brg1^{ep-/-(c)}$ forelimbs from E10 to E12, and in control and $Brg1^{ep-/-(c)}$ hindlimbs at E10 (Fig. 3C, and data not shown). However, at E10.5, *Fgf8* expression in the $Brg1^{ep-/-(c)}$ hindlimbs appeared diffuse, and was patchy as well as drastically reduced at E11.5 (Fig. 3C). At E12, *Fgf8* transcripts were no longer detected in $Brg1^{ep-/-(c)}$ hindlimbs, in contrast to control hindlimbs (data not shown). Histological analysis of E11.5 hindlimbs revealed that the AER of $Brg1^{ep-/-(c)}$ fetuses was highly abnormal. Indeed, cells in the AER region were smaller and much less densely packed than in control foetuses. Their morphology was more similar to neighbouring ectodermal cells (Fig. 3D). Thus, AER formation and maintenance appear normal in forelimbs of $Brg1^{ep-/-(c)}$ fetuses, whereas, in hindlimbs, the AER formation is initiated, but is not maintained from E10.5 onwards, thus resulting in selective hindlimb defects.

Ablation of *Brg1* in keratinocytes of the forming epidermis induces severe skin permeability barrier defects in E18.5 $Brg1^{ep-/-(c)}$ fetuses

Examination of E18.5 mutant fetuses revealed that, in contrast to control animals, their skin was red and glossy, as well as sticky to the touch, and became dry and waxy within 30-45 minutes of cesarian delivery (Fig. 3A, and data not shown). Strikingly, all E18.5 $Brg1^{ep-/-(c)}$ mutants died within 4-6 hours of cesarian delivery, suggesting that their skin permeability barrier could be altered.

To investigate this barrier function, we first determined the diffusion of the fluorescent dye Lucifer Yellow through the

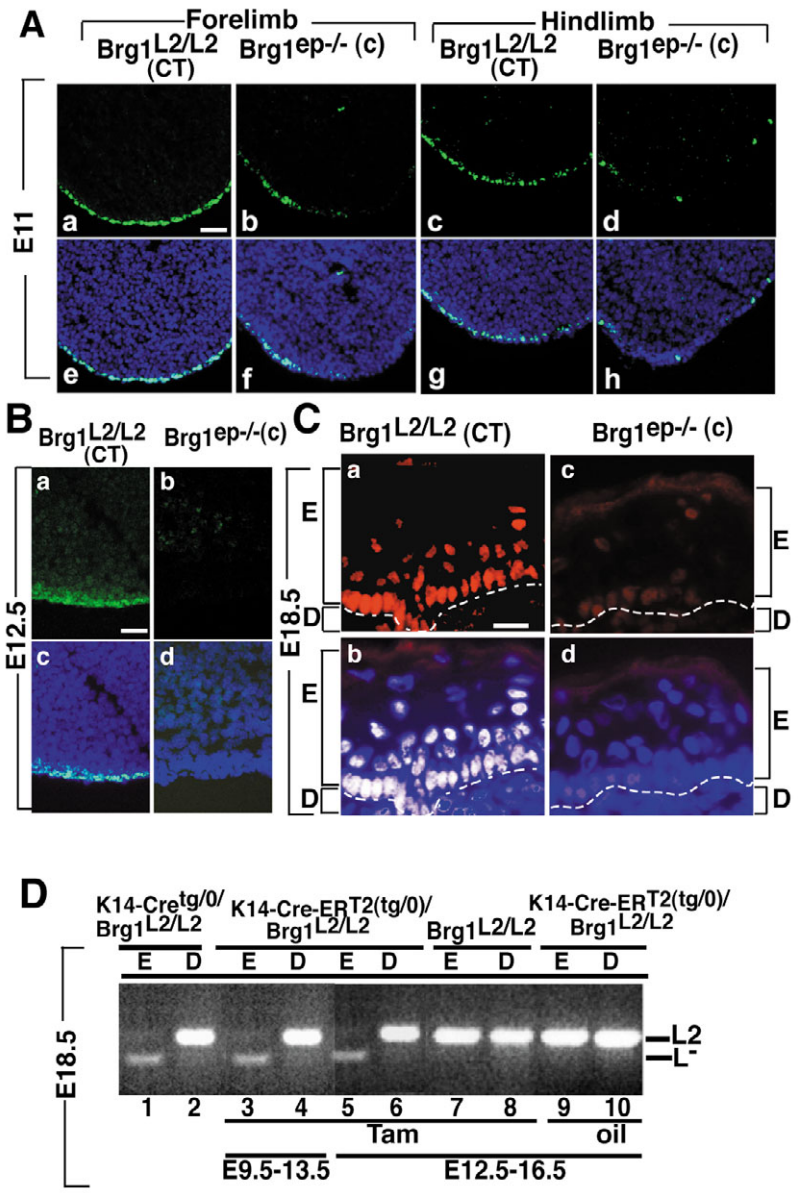

Fig. 2. Selective ablation of BRG1 in the surface ectoderm and epidermal keratinocytes of *K14-Cre*$^{tg/0}$/*Brg1*$^{L2/L2}$ fetuses. (A) Immunohistochemical (IHC) detection (green fluorescence) of *Brg1* (a-h) on E11 forelimb (a,b,e,f) and hindlimb (c,d,g,h) bud tranverse sections from control (a,c,e,g) and *Brg1*$^{ep-/-(c)}$ (b,f,d,h) fetuses. Superimposition of *Brg1* (green fluorescence) and DAPI staining of nuclei (blue fluorescence; e-h). Scale bar in a: 24 μm. (B) IHC detection of *Brg1* on transverse sections through the dorsal ectoderm of E12.5 *Brg1*$^{L2/L2}$ (control; a,c) and *Brg1*$^{ep-/-(c)}$ (b,d) fetuses. Superimposition of *Brg1* (green fluorescence) and DAPI staining of nuclei (blue fluorescence; c,d). Scale bar in a: 24 μm. (C) IHC detection of *Brg1* on dorsal skin sections from (a,b) control *Brg1*$^{L2/L2}$ and (c,d) *Brg1*$^{ep-/-(c)}$ E18.5 fetuses. Red staining corresponds to BRG1 antibody and blue staining to DAPI. E, epidermis; D, dermis. The dotted line indicates the dermal-epidermal junction. Scale bar in a: 10 μm. (D) PCR detection of the *Brg1* L2 and L$^-$ alleles in the epidermis and dermis of E18.5 fetuses. DNA was extracted from tail epidermis (E; lanes 1,3,5,7,9) or dermis (D; lanes 2,4,6,8,10) of fetuses with the indicated genotypes, isolated from females that were Tam treated from either E9.5-E13.5 (lanes 3,4) or E12.5-E16.5 (lanes 5-8), or oil (vehicle) treated from E12.5-E16.5 (lanes 9,10).

skin. As expected the dye was retained in the upper layers of the stratum corneum of E18.5 control fetuses (Matsuki et al., 1998), whereas it diffused in mutant fetuses through the stratum corneum, and was found in the dermis and hypodermis (Fig. 3E, and data not shown). That the barrier function was impaired in the mutants was further supported in fetuses subjected to a whole-mount permeability assay, based on endogenous β-galactosidase activity of skin at low pH (Hardman et al., 1998). As described, E18.5 control fetuses showed very little, if any, X-Gal staining. By contrast, age-matched *Brg1*$^{ep-/-(c)}$ fetuses stained strongly with X-Gal in most regions of the body surface (Fig. 3F). Moreover, E18.5 *Brg1*$^{ep-/-(c)}$ mutant fetuses exhibited a sevenfold higher trans-epidermal water loss (TEWL) in the dorsal and ventral region than control littermates did, and, in contrast to control fetuses, lost 5-10% of their body weight within 4-6 hours of cesarian delivery (Fig. 3G and data not shown).

The epidermis of E18.5 control dorsal skin consisted of a basal layer of dividing cells, two to three layers of spinous and granular cells, and four to six layers of flattened enucleated corneocytes (C) [Fig. 4A, parts a and c, and data not shown (see also Byrne et al., 2003)]. The basal, spinous and granular layers of control and *Brg1*$^{ep-/-(c)}$ skin were similar, but the mutant stratum corneum was flatter (Fig. 4A, compare a and b, and c and d; and data not shown). Hair buds were similarly formed in control and *Brg1*$^{ep-/-(c)}$ skin (Fig. 4A and data not shown). Scanning electron microscopy (SEM) revealed that the folds of dorsal and ventral skin from E18.5 *Brg1*$^{ep-/-(c)}$ fetuses were broader and more disorganised than those of controls (Fig. 4B, and data not shown). Ultrastructural analysis of the epidermis from E18.5 fetuses did not reveal any difference between control and mutant basal and spinous cells (data not shown). Likewise, similar numbers of desmosomes (D), keratohyaline granules (KG), keratin filaments (KF) and lamellar granules (LG; also called keratinosomes) containing packed lipid discs were present in the granular cells of control and mutant mice (Fig. 4C, parts a and b, and data not shown). At the interface of granular and cornified cells of control fetuses, lipid discs extruded from the LG were uniformly aligned and formed lipid lamellar membranes [LL; Fig. 4C, parts c and e; data not shown (see also Downing, 1992; Wertz, 2000)]. By contrast, in mutant epidermis, between granular cells and corneocytes, the lipid discs were replaced by vesicles (marked by arrows in Fig. 4C, parts d,f,h), and the intercellular (lipid) lamellar membranes in cornified layers were disorganised and highly variable in thickness (compare Fig. 4C, parts g and h). When compared with control mice, about fivefold less corneodesmosomes (CD), that were also smaller in size, were present between the mutant cornified cells, and the mutant corneocytes were loosely packed (Fig. 4C, part h, and data not shown).

Immunohistochemical analyses revealed that keratin (K)5 and K14 were similarly expressed in the basal layer of E18.5 control and mutant dorsal epidermis (data not shown). Moreover, the expression patterns of early (K1 and K10 in the spinous layer) and late (loricrin and fillagrin in the granular layer) markers of terminal differentiation were similar in control and mutant dorsal and ventral skin (data not shown). However, Nile Red staining performed on skin sections from E18.5 fetuses revealed that the surface lipid distribution was impaired in mutant fetuses. Indeed, while the neutral lipids formed a yellow-colored dense, continuous ribbon on top of the cornified layer in control fetuses, they were unevenly distributed along the cornified layer of the mutant epidermis (Fig. 5A, compare parts a and b).

Quantitative RT-PCR analyses of the transcription factor KLF4, which is involved in barrier acquisition (Segre et al., 1999), and of claudin 1, a component of tight junctions that is crucial for mammalian epidermal barrier formation (Furuse et al., 2002), revealed similar transcript levels in dorsal skin of E18.5 control and mutant fetuses (Fig. 5B). By contrast, 3- and 1.5-fold reductions in RNA levels of transglutaminase 1 and transglutaminase 3, which encode proteins involved in crosslinking of the stratum corneum (Candi et al., 1995; Kuramoto et al., 2002; Matsuki et al., 1998), were observed in mutant skin (Fig. 5B and data not shown). Moreover, the transcripts of corneodesmosin, which encode a putative adhesion glycoprotein thought to play a key role in the function of corneodesmosomes and thus in corneocyte cohesion (Guerrin et al., 1998), were fourfold lower in mutant than control skin (Fig. 5C).

Taken together, these results demonstrate that the lack of BRG1 in

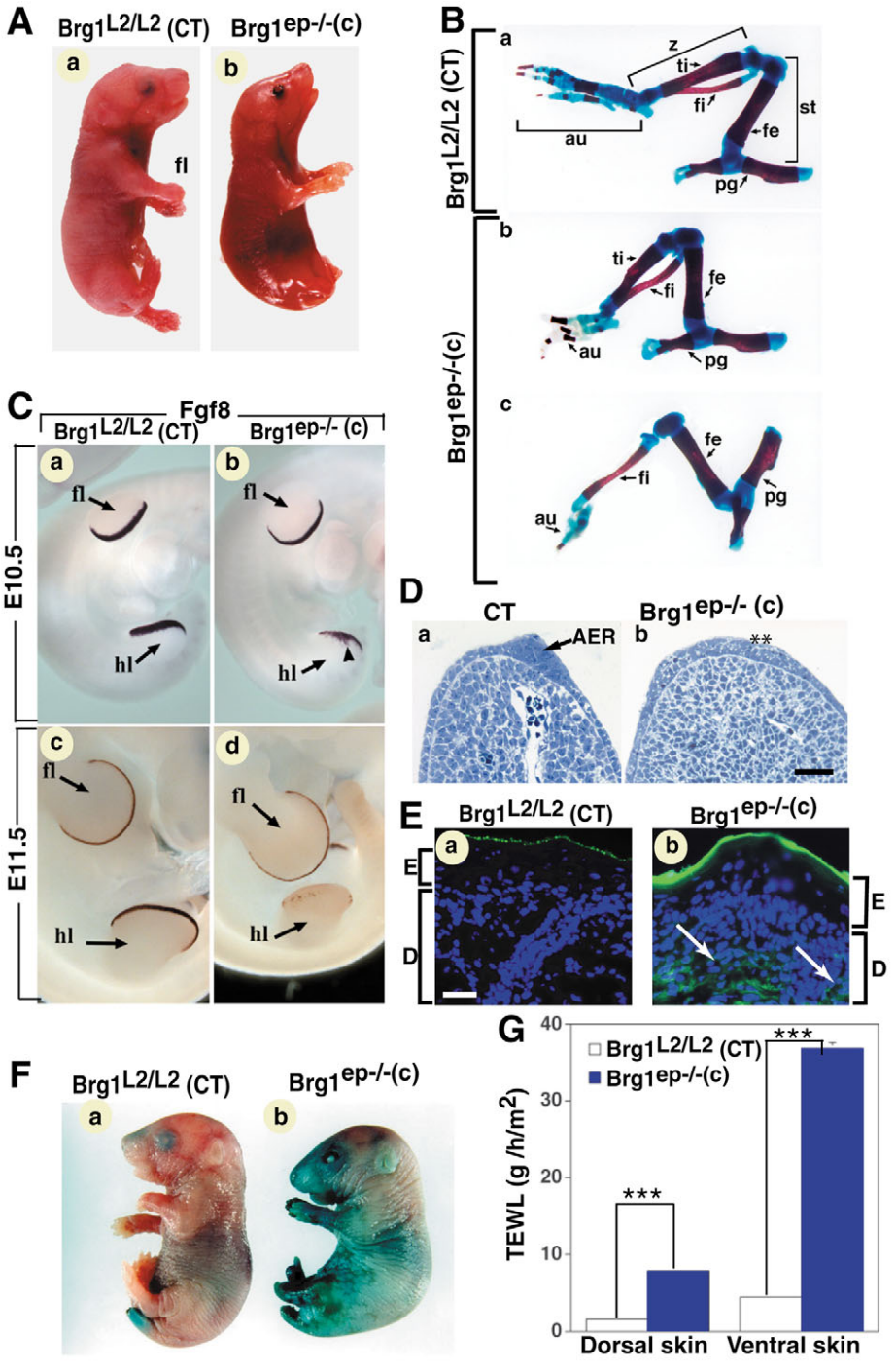

Fig. 3. Morphological and functional analysis of *Brg1*$^{ep-/-(c)}$ mutant fetuses. (A) Gross morphology of *Brg1*$^{L2/L2}$ (control; a) and *Brg1*$^{ep-/-(c)}$ (b) E18.5 fetuses. fl, forelimb. (B) Hindlimb skeletal preparation from *Brg1*$^{L2/L2}$ (a) and *Brg1*$^{ep-/-(c)}$ (b,c) E18.5 fetuses, stained for cartilage (Alcian Blue) and bone (Alizarin Red). Hindlimbs of two different mutants illustrate a mild (b) and the most severe (c) observed malformations. Two (b) and four (c) digits are missing in the autopods (au). The zeugopod (z) exhibits mild deformations of the tibia (ti) and fibula (fi) in b, and lacks the tibia in c. Note that the stylopod (st) and pelvic girdle (pg) are normal. fe, femur. (C) Whole-mount *Fgf8* RNA in situ hybridization in control (a,c) and *Brg1*$^{ep-/-(c)}$ (b,d) fetuses collected at E10.5 (a,b) and E11.5 (c,d). The arrowhead in b points to a mild abnormal domain of *Fgf8* expression at E10.5. fl, forelimb; hl, hindlimb. (D) Anteroposterior transversal semi-thin sections of E11.5 (a) control (CT) and (b) *Brg1*$^{ep-/-(c)}$ mutant hindlimb buds. The AER in control limb bud is indicated by an arrow. **, the altered AER region in the *Brg1*$^{ep-/-(c)}$ mutant limb bud. Scale bar in b: 50 μm. (E) In vivo Lucifer yellow diffusion in (a) *Brg1*$^{L2/L2}$ and (b) *Brg1*$^{ep-/-(c)}$ E18.5 fetuses. Dorsal skin sections were counterstained with DAPI (blue) and analysed by fluorescent microscopy. E, epidermis; D, dermis. Scale bar in a: 33 μm. (F) Barrier-dependent X-Gal diffusion assay on *Brg1*$^{L2/L2}$ (a) and *Brg1*$^{ep-/-(c)}$ (b) E18.5 fetuses. (G) TEWL on dorsal and ventral skin of *Brg1*$^{L2/L2}$ and *Brg1*$^{ep-/-(c)}$ E18.5 fetuses. ***P<0.001.

keratinocytes of the forming epidermis strongly impaired the formation of the skin permeability barrier.

Temporally controlled *Brg1* ablation during epidermis formation

To investigate at which developmental stages BRG1 was required for hindlimb development and skin barrier formation, we performed spatiotemporally controlled *Brg1* ablation, using *K14-Cre-ER*$^{T2(tg/0)}$ transgenic mice that express the tamoxifen (Tam)-activatable Cre-ER^{T2} recombinase under the control of the human *K14* promoter. We previously reported that, upon Tam treatment of this transgenic line, efficient Cre-mediated excision of floxed genes can be induced in keratinocytes of the basal cell layer of the adult epidermis and in the outer root sheath (ORS) of the hair follicle (Indra et al., 2000; Li et al., 2000). To characterise ligand-dependent Cre-mediated recombination in the developing epidermis, *K14-Cre-ER*$^{T2(tg/0)}$ transgenic males were bred with *ROSA*$^{fl/+}$ reporter females. Following tamoxifen administration (0.1 mg) to females at E9.0, *K14-Cre-ER*$^{T2(tg/0)}$/*ROSA*$^{fl/+}$ embryos expressed β-galactosidase at E10.5 in the surface ectoderm of the posterior region, in fore- and hindlimbs, and in pharyngeal arches (Fig. 6A). To analyse Cre-mediated recombination at later stages, 0.1 mg tamoxifen was daily administered to females from either E9.5 to E11.5, E9.5 to E13.5, or E12.5 to E16.5, and fetuses were recovered at E12.5, E14.5 and E18.5, respectively. Skin

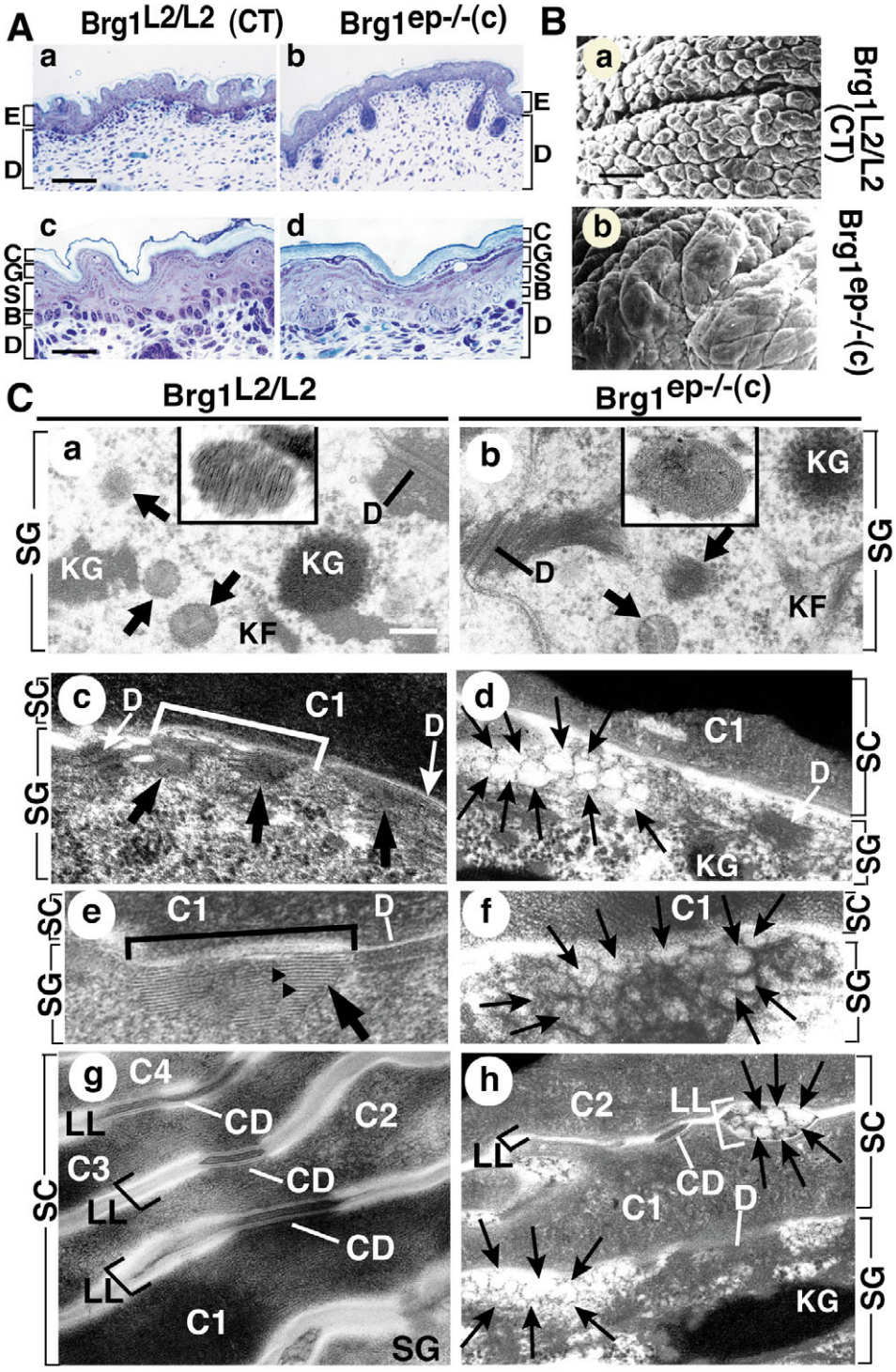

Fig. 4. Characterisation of skin defects in *Brg1*$^{ep-/-(c)}$ fetuses. (A) Histological analysis of Toluidine Blue-stained semithin sections of dorsal skin biopsies from E18.5 *Brg1*$^{L2/L2}$ (a,c) and *Brg1*$^{ep-/-(c)}$ (b,d) fetuses. E, epidermis; D, dermis. Epidermal cell layers are indicated: C, cornified; G, granular; S, spinous; B, basal. Scale bars: in a, 60 μm for a,b; in c, 18 μm for c,d. (B) Scanning electron microscopy of the dorsal skin surface from E18.5 *Brg1*$^{L2/L2}$ (a) and *Brg1*$^{ep-/-(c)}$ (b) fetuses. Scale bar: 10 μm. (C) Transmission electron microscopy of dorsal skin from E18.5 *Brg1*$^{L2/L2}$ (a,c,e,g) and *Brg1*$^{ep-/-(c)}$ (b,d,f,h) fetuses. (a,b) Stratum granulosum (SG). D, desmosomes; KF, keratin filaments; KG, keratohyalin granules. Arrows indicate lamellar granules (LG). Insets show LGs. (c,d,e,f) Junction between stratum granulosum (SG) and stratum corneum (SC). Large black arrows in c and e point towards the LG(s) in the SG-SC interface, and arrowheads in e point towards aligned extracellular lipid discs at the junction between the granular and the cornified layer. The white arrow in c,d indicates desmosomes (D); small black arrows in d,f indicate vesicles at the interface of SG and SC. (g,h) Consecutive C1, C2, C3 and C4 cornified cell layers. Black arrows in h point towards vesicles. Black and white brackets in g and h indicate lipid lamellae (LL). CD, corneodesmosomes. Scale bar in a: 0.2 μm for a,b,c,d; 0.1 μm for e,f; and 0.25 μm for g,h.

sections revealed β-galactosidase activity in most, if not all, epidermal keratinocytes of the *K14-Cre-ER*$^{T2(tg/0)}$/*ROSA*$^{fl/+}$ fetuses analysed. By contrast, no X-Gal staining was observed in *K14-Cre-ER*$^{T2(tg/0)}$/*ROSA*$^{fl/+}$ fetuses from oil (vehicle)-treated females (Fig. 6A,B). These results show that Tam treatment of females during gestation efficiently induced Cre activity in the surface ectoderm and epidermal keratinocytes of fetuses, at various stages of epidermis formation.

To ablate *Brg1* at various times during epidermal morphogenesis, *K14-Cre-ER*$^{T2(tg/0)}$/*Brg1*$^{L2/L2}$ males were bred with *Brg1*$^{L2/L2}$ female mice, from which E18.5 fetuses were recovered after Tam administration at different time points. PCR analyses on skin biopsies of E18.5 fetuses showed efficient conversion of the *Brg1* L2 into the L^{-} allele in the forming epidermis, but not in the dermis, whether Tam was administered to pregnant females from E9.5 to E13.5 or E12.5 to E16.5, thus generating the *Brg1*$^{ep-/-(ia)}$ and *Brg1*$^{ep-/-(ib)}$ fetuses, respectively (Fig. 2D, lanes 3-6, and data not shown). These results show that *Brg1* is efficiently ablated in the proliferating basal keratinocytes that generate the suprabasal keratinocytes of E18.5 fetuses, and therefore in all keratinocytes of *Brg1*$^{ep-/-(ia)}$ and *Brg1*$^{ep-/-(ib)}$ fetuses at E18.5. By contrast, no *Brg1* ablation was observed in control *Brg1*$^{L2/L2}$ littermates, or in *K14-Cre-ER*$^{T2(tg/0)}$/*Brg1*$^{L2/L2}$ fetuses from oil (vehicle)–treated females (Fig. 2D, lanes 7–10, and data not shown).

Like *Brg1*$^{ep-/-(c)}$ fetuses, E18.5 *Brg1*$^{ep-/-(ia)}$ mutant fetuses (Tam administration from E9.5 to 13.5) exhibited severe hindlimb and tail malformations (whereas forelimbs were unaffected), and died within 4-6 hours of cesarian delivery (Fig. 7A, part b, and data not shown). Moreover, skin defects similar to those of *Brg1*$^{ep-/-(c)}$ fetuses (Fig. 4A-C), i.e. flattening of skin, absence of corneodesmosomes, defects in the alignment of lamellar bodies were observed (data not shown). In marked contrast, when Tam was administered to females from 12.5-16.5 days of gestation, hindlimbs and tails were unaffected in the corresponding E18.5 *Brg1*$^{ep-/-(ib)}$ fetuses (see Fig. 7A, part d), which, however, exhibited impaired skin barrier function, lost 5-10% of their body weight within 4-6 hours of cesarian delivery, and died (Fig. 7D,E, and data not shown). These *Brg1*$^{ep-/-(ib)}$ mutant fetuses exhibited similar skin defects as *Brg1*$^{ep-/-(c)}$ and *Brg1*$^{ep-/-(ia)}$ mutants (Fig. 7B,C, and data not shown). Importantly, E18.5 *Brg1*$^{L2/L2}$ fetuses from Tam- or vehicle-treated females had no limb and skin defects (see Fig. 7A, parts a and c, and data not shown).

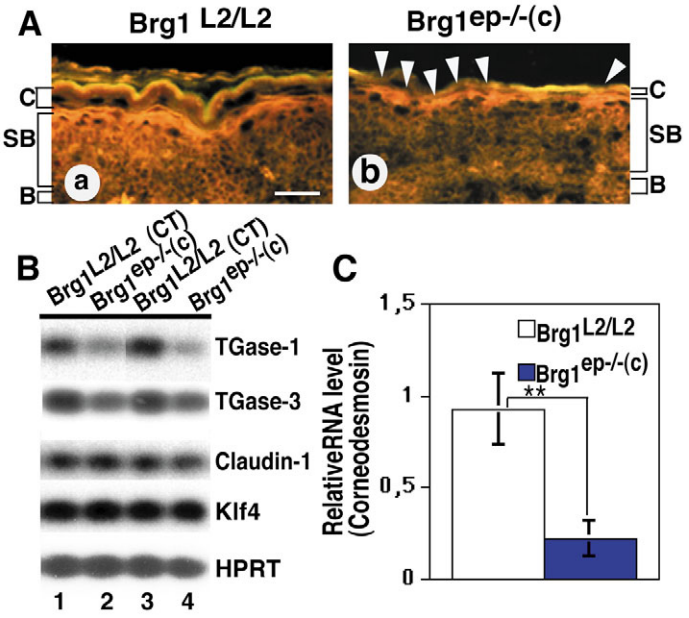

Fig. 5. Staining for neutral lipids and analysis of genes involved in epidermal barrier formation in skin from *Brg1*$^{ep-/-(c)}$ fetuses. (A) Nile Red staining for neutral lipids in the skin of E18.5 control (a) and *Brg1*$^{ep-/-(c)}$ fetuses (b). Arrowheads in b indicate an absence of neutral lipids. Scale bar in a: 16 μm. C, cornified layer; SB, suprabasal layer; B, basal layer. (B) Quantitative RT-PCR analysis of skin RNA from E18.5 *Brg1*$^{L2/L2}$ (lanes 1 and 3) and *Brg1*$^{ep-/-(c)}$ (lanes 2 and 4) fetuses. (C) Real-time RT-PCR analysis of corneodesmosin on skin RNA from E18.5 *Brg1*$^{L2/L2}$ and *Brg1*$^{ep-/-(c)}$ fetuses. $^{**}P<0.001$.

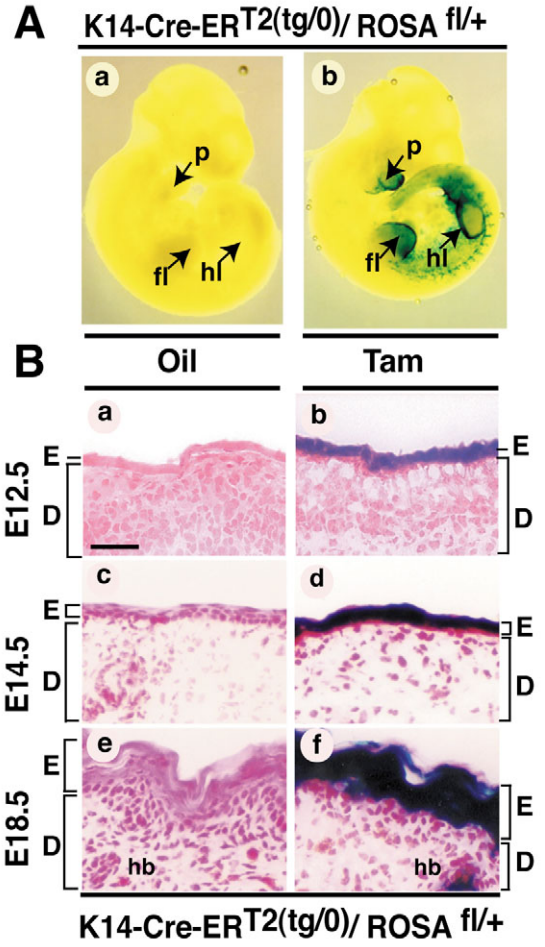

Fig. 6. Characterization of Tam-induced Cre recombinase activity in the surface ectoderm and forming epidermis of *K14-Cre-ER*^{T2} transgenic mice. (A) Whole-mount X-Gal-stained E10.5 *K14-Cre-ER*$^{T2(tg/0)}$/*ROSA*$^{fl/+}$ embryo after (a) oil and (b) 0.1 mg Tam injection to a female at E9.0. fl, forelimb; hl, hindlimb; p, first pharyngeal arch. (B) X-Gal-stained dorsal skin sections of E12.5 (a,b), E14.5 (c,d) and E18.5 (e,f) *K14-Cre-ER*$^{T2(tg/0)}$/*ROSA*$^{fl/+}$ fetuses after daily injections of oil (a,c,e) or Tam (b,d,f) to females from E9.5-E11.5 (a,b), E 9.5-E13.5 (c,d) and E12.5-E16.5 (e,f) days gestation. Sections were counterstained with safranin. E, epidermis; D, dermis; hb, hair bulb. Scale bar in a: 16 μm.

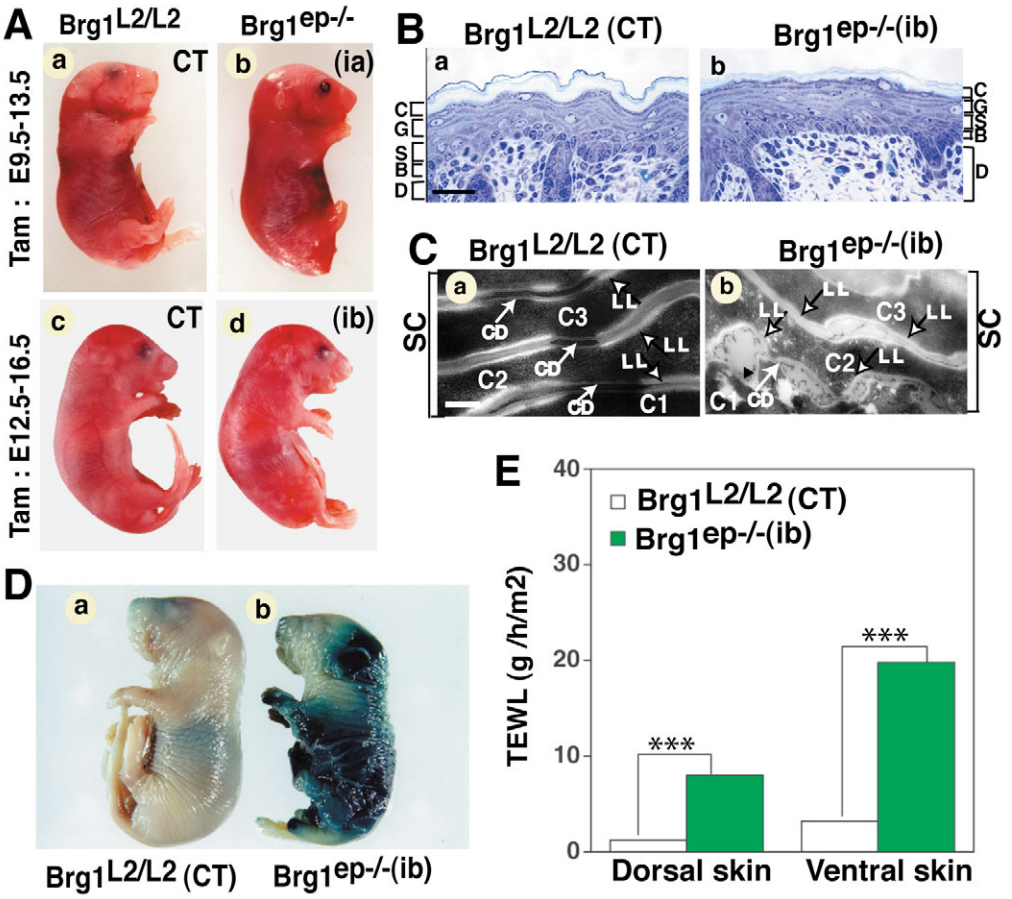

Fig. 7. Characterisation of fetuses after temporally controlled *Brg1* ablation in the forming epidermis. (A) Gross morphology of (a,c) control $Brg1^{L2/L2}$, (b) $Brg1^{ep-/-(ia)}$ and (d) $Brg1^{ep-/-(ib)}$ E18.5 fetuses after daily Tam administration to pregnant females from E9.5-E13.5 (a,b) and E12.5-E16.5 (c,d). (B) Histological analysis of Toluidine Blue-stained semithin sections of dorsal skin biopsies from (a) control $Brg1^{L2/L2}$ and (b) $Brg1^{ep-/-(ib)}$ E18.5 fetuses. C, cornified layer; G, granular layer; S, suprabasal layer; B, basal layer; D, dermis. Scale bar in a: 18 μm. (C) Transmission electron microscopy of stratum corneum (SC) (C1,C2 and C3 consecutive cornified cell layers) from dorsal skin of (a) $Brg1^{L2/L2}$ and (b) $Brg1^{ep-/-(ib)}$ E18.5 fetuses. White arrows and white arrowheads point towards corneodesmosomes (CD) and lipid lamellae (LL), respectively. Scale bar in a: 0.25 μm. (D) X-Gal diffusion assay on (a) control $Brg1^{L2/L2}$ and (b) $Brg1^{ep-/-(ib)}$ mutant E18.5 fetuses. (E) TEWL measured on E18.5 control $Brg1^{L2/L2}$ and $Brg1^{ep-/-(ib)}$ fetuses. ***P<0.001.

Partial functional redundancy between *Brm* and *Brg1* for terminal epidermal keratinocyte differentiation

To investigate whether *Brm*, which is mainly expressed in suprabasal cells of the forming interfollicular epidermis (see Fig. S1A in the supplementary material), could compensate BRG1 functions in *Brg1*-lacking keratinocytes, *Brg1* was selectively ablated during skin formation in keratinocytes of $Brm^{-/-}$ mice, through Tam administration from E12.5-E16.5 to gestating $Brm^{+/-}/Brg1^{L2/L2}$ females that were bred with *K14-Cre-ER*$^{T2(tg/0)}$/$Brm^{-/-}/Brg1^{L2/L2}$ males. Note that E18.5 $Brm^{-/-}$ fetuses were indistinguishable from their wild-type ($Brm^{+/+}$) or heterozygous ($Brm^{+/-}$) littermates (see Fig. S1B in the supplementary material, and data not shown). Moreover, light and electron microscopy of their skin did not reveal any difference, and their skin permeability barrier function, as determined by X-Gal diffusion, was similar (Fig. S1C-E in the supplementary material, and data not shown).

E18.5 $Brm^{-/-}/Brg1^{ep-/-(ib)}$ fetuses had normal fore- and hindlimbs, and their skin was formed (Fig. 8A,B, and data not shown). Moreover, they exhibited a similar basal cell proliferation rate to control and $Brg1^{ep-/-(c)}$ fetuses, as determined by immunohistochemical detection of Ki67 [a nuclear protein expressed in proliferating cells (Schlüter et al., 1993)] (Fig. 8C,D). However, their spinous and granular cells displayed swollen cytoplasm and nuclei, and only one to two cornified cell layer(s) were present (Fig. 8B,E, and data not shown). Moreover, their skin permeability barrier function was more affected than that of $Brg1^{ep-/-(ib)}$ fetuses (Fig. 8F,G). Thus, keratinocytes lacking both BRM and BRG1 can proliferate and differentiate to some extent, and even though BRM does not play any essential role in suprabasal cells, it is partially redundant with BRG1 in these cells.

Discussion

Ablation of *Brg1* in the forming epidermis does not affect the proliferation and early differentiation of keratinocytes, but does induce severe skin permeability barrier defects

Although the BRG1 protein is expressed in the forming epidermis before keratinocytes enter early terminal differentiation, and is expressed mainly in basal keratinocytes at later stages of epidermal maturation, we show here that the selective Cre-mediated ablation of *Brg1* in the surface ectoderm at E12.5 and in epidermal keratinocytes does not affect epidermal keratinocyte proliferation. This is in contrast with its absolute requirement for the proliferation of F9 embryonal carcinoma cells and the cells of preimplantation embryos (Bultman et al., 2000; Sumi-Ichinose et al., 1997), thus demonstrating that there is a cell type-specific differential requirement of BRG1-containing chromatin remodelling complexes to regulate cell proliferation in vivo.

Conversely, keratinocytes lacking *Brg1* undergo normal stratification, but their late terminal differentiation is severely impaired. Apparently normal lamellar granules (LG)

containing lipid discs were present in *Brg1*-null granular cells, but extrusion of their lipid content at the interfaces between granular and cornified cells was altered, resulting in disorganised lipid multi-lamellar structures in the stratum corneum, and uneven neutral lipid distribution. This defective processing might be caused by an altered lipid composition

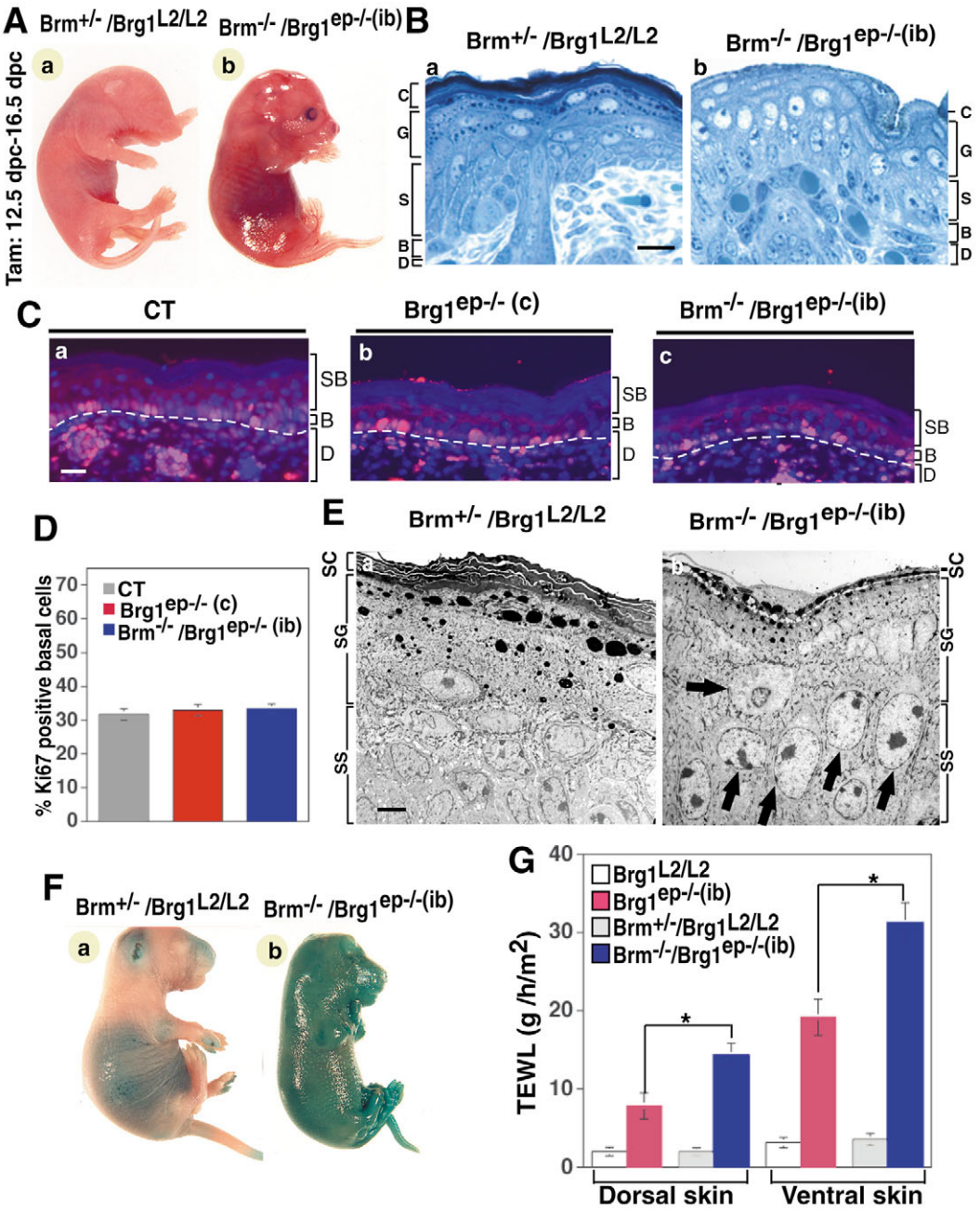

Fig. 8. Morphological and functional analysis of $Brm^{-/-}/Brg1^{ep-/-(ib)}$ mutant fetuses. (A) Gross morphology of (a) $Brm^{+/-}/Brg1^{L2/L2}$ and (b) $Brm^{-/-}/Brg1^{ep-/-(ib)}$ E18.5 fetuses. (B) Histological analysis of Toluidine Blue-stained semithin sections of dorsal skin biopsies from E18.5 $Brm^{+/-}/Brg1^{L2/L2}$ (a) and $Brm^{-/-}/Brg1^{ep-/-(ib)}$ (b) fetuses. Epidermal cell layers are indicated: C, cornified; G, granular; S, spinous; B, basal; D, dermis. Scale bar in a: 12 μm. (C) Immunohistochemical detection of proliferation marker KI67 (pink colour) on dorsal skin sections from E18.5 control (a), $Brg1^{ep-/-(c)}$ (b) and $Brm^{-/-}/Brg1^{ep-/-(ib)}$ (c) fetuses. Nuclei are stained with DAPI (blue). B, basal; SB, suprabasal; D, dermis. Scale bar in a: 25 μm. The dotted line indicates the dermal-epidermal junction. (D) Percentage of KI67-positive basal cells in the dorsal skin of E18.5 control, $Brg1^{ep-/-(c)}$ and $Brm^{-/-}/Brg1^{ep-/-(ib)}$ fetuses. The number of KI67-positive cells out of 3000 DAPI-stained interfollicular basal cells were determined on four 10-μm thick frozen skin sections from three controls and three mutants. Values expressed as a percentage are the mean values±s.e.m. (n=12). (E) Transmission electron microscopy of dorsal skin from E18.5 $Brm^{+/-}/Brg1^{L2/L2}$ (a) and $Brm^{-/-}/Brg1^{ep-/-(ib)}$ (b) fetuses. SC, stratum corneum; SG, stratum granulosum; SS, stratum spinosum. Arrows point to swollen cells in the spinous and granular layers. Scale bar: 4 μm. (F) Barrier-dependent X-Gal diffusion assay on E18.5 $Brm^{+/-}/Brg1^{L2/L2}$ (a) and $Brm^{-/-}/Brg1^{ep-/-(ib)}$ (b) fetuses. (G) TEWL on dorsal and ventral skin of E18.5 $Brg1^{L2/L2}$, $Brg1^{ep-/-(ib)}$, $Brm^{+/-}/Brg1^{L2/L2}$ and $Brm^{-/-}/Brg1^{ep-/-(ib)}$ fetuses. *P<0.05.

and/or protein content in the lamellar granules. Moreover, the size and number of corneodesmosomes, which physically hold the cells together in the stratum corneum, was markedly reduced, and thus might be the basis of a reduced cohesion of the stratum corneum. The decrease in corneodesmosome density in the lower cornified layers might result from an impaired transfer of proteins from the lamellar granules into desmosomes, including corneodesmosin (Lundstrom et al., 1994), whose transcripts were reduced in *Brg1* mutant mice. As transglutaminase 1 (*TGase1*) and transglutaminase 3 (*TGase3*) transcripts were also reduced in fetal *Brg1* mutant skin, crosslinking of proteins might also be impaired in the statum corneum. Together, these defects account for the defective skin permeability barrier function and lead to an early postnatal death.

Although the three essential processes required to establish epidermal permeability barrier functions [(1) extrusion of LG lipid contents at the interface of granular and cornified cells, (2) integrity of the corneodesmosomes in the lipid lamellar bilayer and (3) normal expression levels of transglutaminase 1 and 3 to crosslink the stratum corneum envelope proteins] were impaired, not all genes involved in epidermal terminal differentiation were affected. Indeed, claudin and *Klf4* transcript levels, as well as fillagrin, loricrin and involucrin protein expression patterns and/or levels, were similar in control and mutant epidermis. Thus BRG1-containing chromatin remodelling complexes control the expression of a restricted subset of genes required for the establishment of the skin barrier during late gestation. Moreover, as Tam-induced *Brg1* ablation after E12.5 in the forming epidermis of *K14-Cre-ER*$^{T2(tg/0)}$/*Brg1*$^{L2/L2}$ (*Brg1*$^{ep-/-(ib)}$) fetuses resulted in similar epidermal defects to those of *Brg1*$^{ep-/-(c)}$ fetuses in which *Brg1* is ablated in the surface ectoderm at an earlier time, our present data demonstrate that this crucial control by BRG1-containing complexes is exerted during late stratification and/or terminal keratinocyte differentiation.

Interestingly, keratinocyte proliferation and stratification occur normally in *Brm*$^{-/-}$/*Brg1*$^{ep-/-(ib)}$ fetal skin, in which *Brg1* is ablated in *Brm*$^{-/-}$ keratinocytes after E12.5, which indicates that SWI2/SNF2 protein complexes are not essential for basal cell proliferation and/or early differentiation. However, even though the epidermis of *Brm* null fetuses appears normal, more severe defects were observed in suprabasal cells of *Brm*$^{-/-}$/*Brg1*$^{ep-/-(ib)}$ fetuses than in those of *Brg1*$^{ep-/-(ib)}$ fetuses. Thus, BRM can partially substitute for BRG1 functions in these cells.

Taken together, our data indicate that BRG1-selective control of gene expression in the epidermal keratinocyte lineage is restricted to its terminal stages of differentiation, and that BRM is partially redundant with BRG1.

Brg1 ablation in the limb ectoderm induces hindlimb defects

We have shown here that *Brg1* ablation in the limb ectoderm of *K14-Cre*/*Brg1*$^{L2/L2}$ [*Brg1*$^{ep-/-(c)}$] embryos induces severe hindlimb defects. The AER is known to be essential at early stages of limb development to establish appropriately sized progenitor cell populations for the proximal (stylopod), middle (zeugopod) and distal (autopod) segments. Surgical removal of the AER from an early developing limb bud results in the loss of almost all limb structures, whereas its removal at later stages results in progressively more distal losses, while proximal structures are unaffected (Summerbell, 1974). Similarly, early genetic ablation of both *Fgf4* and *Fgf8* results in a complete failure of limb development, whereas later inactivation of *Fgf4* and *Fgf8* results in the production of all segments along the proximodistal axis, but with distal segments that are reduced in size and number (Sun et al., 2002).

In *Brg1*$^{ep-/-(c)}$ conditional mutants, in which *Brg1* was ablated in the limb surface ectoderm around E11, the skeletal elements derived from the proximal hindlimb segment developed normally, but those derived from the zeugopod and autopod were severely hypoplastic or absent. Interestingly, the expression of *Fgf8*, a key factor for AER function, which was initially similar in the hindlimb buds of control and *Brg1*$^{ep-/-(c)}$ embryos, was progressively affected by E10.5, and disappeared in *Brg1*$^{ep-/-(c)}$ embryos at E12. In this respect, we note that although *Fgf8* expression was already severely altered at E10.5, BRG1 protein levels were strongly decreased by E11 only. Thus, it appears that a moderate reduction of BRG1 levels could be sufficient to impair FGF8 production, and therefore AER maintenance. Altogether, our results show that BRG1 activity is essential in the hindlimb ectoderm for the maintenance of the AER, most probably through the regulation of *Fgf8* signaling (Sun et al., 2002).

Surprisingly, *Fgf8* was normally expressed in *Brg1*$^{ep-/-(c)}$ forelimbs, which developed properly, even though the expression of BRG1 was sharply decreased in about 70% of the cells of the forelimb surface ectoderm at E11.0, and was undetectable at E11.5. Thus *Brg1* might only be required for forelimb AER maintenance and *Fgf8* expression during a limited time period, before E10.5-E11.5. Interestingly, temporally controlled *Brg1* ablation in the surface ectoderm by Tam-treatment of females from E9.5 to E13.5 similarly resulted in hindlimb, but not forelimb defects. By contrast, ablation of *Brg1* in the forming epidermis at later time (Tam treatment from E12.5 to E16.5) did not induce any limb defect, indicating that *Brg1* plays a crucial role during limb morphogenesis in a narrow temporal window. The absence of forelimb abnormalities probably reflects differences in the timing of *Brg1* ablation in the forelimb and in the hindlimb, rather than a differential involvement of *Brg1* in fore- and hindlimb development. Forelimb bud formation is induced at E9, i.e. 24 hours earlier than hindlimb bud formation (Kaufman and Bard, 1999), and our data indicate that during this time period Cre-mediated DNA excision is more efficient in the surface ectoderm of the posterior part of the embryo.

Conclusion

Taken together, our results indicate that *Brg1* controls selectively the expression of genes involved in the epithelial-mesenchymal interactions required for limb patterning (Byrne et al., 2003) and in terminal keratinocyte differentiation during epidermal histogenesis. As it is the case for undifferentiated F9 embryonal carcinoma cells and in peri-implantation embryos (Bultman et al., 2000; Sumi-Ichinose et al., 1997), BRM, which is dispensable for epidermis and limb formation, cannot functionally replace BRG1 in these processes. However BRM can partially substitute for BRG1 in keratinocytes undergoing terminal differentiation. Importantly, as keratinocytes lacking both BRM and BRG1 in developing fetuses proliferate and undergo early differentiation, it appears that some cellular programs do not require SWI2/SNF2-containing chromatin

remodelling complexes. Rather, they might be controlled by ATP-dependent nucleosome remodelling complexes containing other members of the SNF2 subfamilies, such as ISWI or Mi-2. Last but not least, the present study demonstrates that, using Cre-ER^{T2}-mediated recombination, cell-specific targeted somatic mutations can be created at various times during the development of the mouse embryo, making possible to dissect gene function throughout morphogenesis.

We are grateful to P. Soriano for Rosa R26R mice, to G. Martin for the *Fgf8* probe and to C. Sumi-Ichinose for the pSNF2β$^{L:LHLa}$ targeting vector. We thank Dr Filippo Rijli for helpful discussion, R. Lorentz, B. Chofflet, C. Dennefeld and M. Duval for excellent technical help, E. Metzger and the animal facility staff for animal care, A. Dierich for ES cell culture, and the secretarial and the illustration staff for preparing the manuscript. This work was supported by funds from the Human Frontier Science Program, the Centre National de la Recherche Scientifique, the Institut National de la Santé et de la Recherche Médicale, the Collège de France, the Association pour la Recherche Médicale, the Ministère de l'Education Nationale de la Recherche et de la Technologie, and the European Community.

Supplementary material

Supplementary material for this article is available at
http://dev.biologists.org/cgi/content/full/132/20/4533/DC1

References

Bultman, S., Gebuhr, T., Yee, D., La Mantia, C., Nicholson, J., Gilliam, A., Randazzo, F., Metzger, D., Chambon, P., Crabtree, G. et al. (2000). A Brg1 null mutation in the mouse reveals functional differences among mammalian SWI/SNF complexes. *Mol. Cell* **6**, 1287-1295.

Byrne, C., Tainsky, M. and Fuchs, E. (1994). Programming gene expression in developing epidermis. *Development* **120**, 2369-2383.

Byrne, C., Hardman, M. and Nield, K. (2003). Covering the limb–formation of the integument. *J. Anat.* **202**, 113-123.

Candi, E., Melino, G., Mei, G., Tarcsa, E., Chung, S. I., Marekov, L. N. and Steinert, P. M. (1995). Biochemical, structural, and transglutaminase substrate properties of human loricrin, the major epidermal cornified cell envelope protein. *J. Biol. Chem.* **270**, 26382-26390.

Chi, T. H., Wan, M., Lee, P. P., Akashi, K., Metzger, D., Chambon, P., Wilson, C. B. and Crabtree, G. R. (2003). Sequential roles of Brg, the ATPase subunit of BAF chromatin remodeling complexes, in thymocyte development. *Immunity* **19**, 169-182.

Choi, D. S., Ward, S. J., Messaddeq, N., Launay, J. M. and Maroteaux, L. (1997). 5-HT2B receptor-mediated serotonin morphogenetic functions in mouse cranial neural crest and myocardiac cells. *Development* **124**, 1745-1755.

Dierich, A. and Dollé, P. (1997). Gene targeting in embryonic stem cells. In *Methods in Development Biology/Toxicology* (ed. S. Klug and R. Thiel), pp. 111-123: Oxford: Blackwell.

Downing, D. T. (1992). Lipid and protein structures in the permeability barrier of mammalian epidermis. *J. Lipid Res.* **33**, 301-313.

Eberharter, A. and Becker, P. B. (2004). ATP-dependent nucleosome remodelling: factors and functions. *J. Cell Sci.* **117**, 3707-3711.

Furuse, M., Hata, M., Furuse, K., Yoshida, Y., Haratake, A., Sugitani, Y., Noda, T., Kubo, A. and Tsukita, S. (2002). Claudin-based tight junctions are crucial for the mammalian epidermal barrier: a lesson from claudin-1-deficient mice. *J. Cell Biol.* **156**, 1099-1111.

Guerrin, M., Simon, M., Montezin, M., Haftek, M., Vincent, C. and Serre, G. (1998). Expression cloning of human corneodesmosin proves its identity with the product of the S gene and allows improved characterization of its processing during keratinocyte differentiation. *J. Biol. Chem.* **273**, 22640-22647.

Hardman, M. J., Sisi, P., Banbury, D. N. and Byrne, C. (1998). Patterned acquisition of skin barrier function during development. *Development* **125**, 1541-1552.

Indra, A. K., Warot, X., Brocard, J., Bornert, J. M., Xiao, J. H., Chambon, P. and Metzger, D. (1999). Temporally-controlled site-specific mutagenesis in the basal layer of the epidermis: comparison of the recombinase activity of the tamoxifen-inducible Cre-ER(T) and Cre-ER(T2) recombinases. *Nucleic Acids Res.* **27**, 4324-4327.

Indra, A. K., Li, M., Brocard, J., Warot, X., Bornert, J. M., Gérard, C., Messaddeq, N., Chambon, P. and Metzger, D. (2000). Targeted somatic mutagenesis in mouse epidermis. *Horm. Res.* **54**, 296-300.

Kadam, S. and Emerson, B. M. (2003). Transcriptional specificity of human SWI/SNF BRG1 and BRM chromatin remodeling complexes. *Mol. Cell* **11**, 377-389.

Kalinin, A. E., Kajava, A. V. and Steinert, P. M. (2002). Epithelial barrier function: assembly and structural features of the cornified cell envelope. *BioEssays* **24**, 789-800.

Kaufman, M. H. and Bard, J. B. L. (1999). *The Anatomical Basis of Mouse Development*. San Diego, USA: Academic Press.

Kuramoto, N., Takizawa, T., Matsuki, M., Morioka, H., Robinson, J. M. and Yamanishi, K. (2002). Development of ichthyosiform skin compensates for defective permeability barrier function in mice lacking transglutaminase 1. *J. Clin. Invest.* **109**, 243-250.

Li, M., Indra, A. K., Warot, X., Brocard, J., Messaddeq, N., Kato, S., Metzger, D. and Chambon, P. (2000). Skin abnormalities generated by temporally controlled RXRalpha mutations in mouse epidermis. *Nature* **407**, 633-636.

Li, M., Chiba, H., Warot, X., Messaddeq, N., Gerard, C., Chambon, P. and Metzger, D. (2001). RXR-alpha ablation in skin keratinocytes results in alopecia and epidermal alterations. *Development* **128**, 675-688.

Lufkin, T., Mark, M., Hart, C. P., Dollé, P., LeMeur, M. and Chambon, P. (1992). Homeotic transformation of the occipital bones of the skull by ectopic expression of a homeobox gene. *Nature* **359**, 835-841.

Lundstrom, A., Serre, G., Haftek, M. and Egelrud, T. (1994). Evidence for a role of corneodesmosin, a protein which may serve to modify desmosomes during cornification, in stratum corneum cell cohesion and desquamation. *Arch. Dermatol. Res.* **286**, 369-375.

Matsuki, M., Yamashita, F., Ishida-Yamamoto, A., Yamada, K., Kinoshita, C., Fushiki, S., Ueda, E., Morishima, Y., Tabata, K., Yasuno, H. et al. (1998). Defective stratum corneum and early neonatal death in mice lacking the gene for transglutaminase 1 (keratinocyte transglutaminase). *Proc. Natl. Acad. Sci. USA* **95**, 1044-1049.

Metzger, D., Indra, A. K., Li, M., Chapellier, B., Calleja, C., Ghyselinck, N. B. and Chambon, P. (2003). Targeted conditional somatic mutagenesis in the mouse: temporally-controlled knock out of retinoid receptors in epidermal keratinocytes. *Methods Enzymol.* **364**, 379-408.

Moon, A. M. and Capecchi, M. R. (2000). Fgf8 is required for outgrowth and patterning of the limbs. *Nat. Genet.* **26**, 455-459.

Reyes, J. C., Barra, J., Muchardt, C., Camus, A., Babinet, C. and Yaniv, M. (1998). Altered control of cellular proliferation in the absence of mammalian brahma (SNF2alpha). *EMBO J.* **17**, 6979-6991.

Schlüter, C., Duchrow, M., Wohlenberg, C., Becker, M. H. G., Key, G., Flad, H.-D. and Gerdes, F. (1993). The cell proliferation-associated antigen of antibody Ki-67: a very large, ubiquitous nuclear protein with numerous repeated elements, representing a new kind of cell-cycle maintaining proteins. *J. Cell Biol.* **123**, 513-522.

Segre, J. A., Bauer, C. and Fuchs, E. (1999). Klf4 is a transcription factor required for establishing the barrier function of the skin. *Nat. Genet.* **22**, 356-360.

Soriano, P. (1999). Generalized lacZ expression with the ROSA26 Cre reporter strain. *Nat. Genet.* **21**, 70-71.

Sumi-Ichinose, C., Ichinose, H., Metzger, D. and Chambon, P. (1997). SNF2beta-BRG1 is essential for the viability of F9 murine embryonal carcinoma cells. *Mol. Cell. Biol.* **17**, 5976-5986.

Summerbell, D. (1974). A quantitative analysis of the effect of excision of the AER from the chick limb-bud. *J. Embryol. Exp. Morphol.* **32**, 651-660.

Sun, X., Mariani, F. V. and Martin, G. R. (2002). Functions of FGF signalling from the apical ectodermal ridge in limb development. *Nature* **418**, 501-508.

Vassar, R., Rosenberg, M., Ross, S., Tyner, A. and Fuchs, E. (1989). Tissue-specific and differentiation-specific expression of a human K14 keratin gene in transgenic mice. *Proc. Natl. Acad. Sci. USA* **86**, 1563-1567.

Watt, F. M. (2000). Epidermal stem cells as targets for gene transfer. *Hum. Gene. Ther.* **11**, 2261-2266.

Wendling, O., Ghyselinck, N. B., Chambon, P. and Mark, M. (2001). Roles of retinoic acid receptors in early embryonic morphogenesis and hindbrain patterning. *Development* **128**, 2031-2038.

Wertz, P. W. (2000). Lipids and barrier function of the skin. *Acta Derm. Venereol. Suppl.* **208**, 7-11.

Table S1. Frequency of the various hindlimb phenotypes observed in E18.5 *Brg1*$^{ep-/-}$ fetuses

Hindlimb	Wild type (*n*=16)	*Brg1*$^{ep-/-}$ (*n*=12)
Normal	100%	0%
Normal tibia and three to five digits*	0%	25%
Truncated tibia and four or five digits*	0%	25%
Truncated tibia and only one to three digits*	0%	25%
No tibia and only one digit*	0%	25%

*Abnormal digit.